Supplement of Atmos. Chem. Phys., 18, 2853–2881, 2018
https://doi.org/10.5194/acp-18-2853-2018-supplement
© Author(s) 2018. This work is distributed under
the Creative Commons Attribution 4.0 License.

Atmospheric Chemistry and Physics
Open Access

Supplement of

Long-term cloud condensation nuclei number concentration, particle number size distribution and chemical composition measurements at regionally representative observatories

Julia Schmale et al.

Correspondence to: Julia Schmale (julia.schmale@gmail.com) and Martin Gysel (martin.gysel@psi.ch)

The copyright of individual parts of the supplement might differ from the CC BY 4.0 License.

1 Data corrections

Jungfraujoch (JFJ) CCN data

The operation and data analyses procedures for the SMPS at JFJ are described in detail in Jurányi et al. (2011) and Herrmann et al. (2015). Routinely, the integrated SMPS particle number concentration is compared to a reference CPC. Discrepancies of greater than 20 % in concentrations are removed from any further data analysis.

At a supersaturation of 1.0 % it is expected that all particles activate if the number fraction of particles with a diameter lower than 30 nm is small (e.g., Schmale et al., 2017). We calculate the total number concentrations of particles > 30 nm (CN_{30}) from the SMPS data and compare them to the $CCN_{1.0}$ number concentration for the years 2012 through 2014, see Fig. S1. Discrepancies in 2012 and 2013 are beyond the 10 % counting uncertainty of both the SMPS and CCNC (compare the black solid and dashed lines with the color coded data points). In 2012 the CCNC significantly underestimated the CCN number concentration while in 2013 it overestimated it. This is likely due to the malfunctioning of the humidifying membrane in the CCNC which was replaced at the end of 2012 due to underreporting. The new membrane did not operate properly until late in 2013, hence the discrepancy in 2013. In 2014 the CCNC operated correctly as can be seen in the figure. Based on closure attempts following the κ-Köhler theory as described in Section 2.3.2 in the manuscript the concentration biases in 2012 and 2013 were found to be independent of the applied supersaturation. For the data analysis presented in the manuscript, the CCN number concentrations were corrected accordingly.

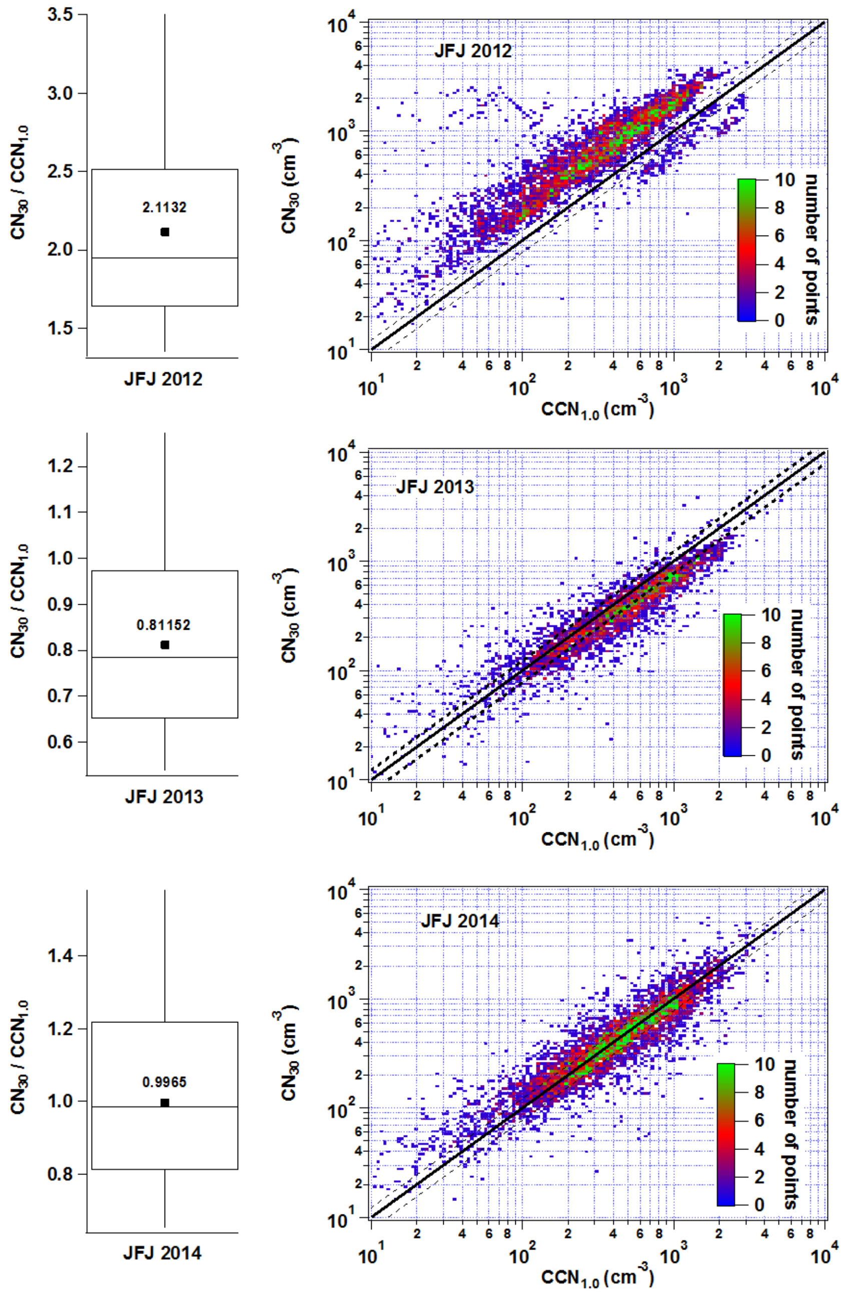

Fig. S1: Untreated JFJ data from 2012, 2013 and 2014. The left panels show the ratio of the total particle number > 30 nm and the CCN number concentration at SS = 1.0 % as a box and whiskers plot. The box indicates the interquartile range, the whiskers the 10th and 90th percentiles, the middle horizontal bar the median and the marker the geometric mean whose value is also given. The right panels show the relationship between CN_{30} and $CCN_{1.0}$ within logarithmic bins. The color code indicates the number of particles falling within one bin space. The solid black line is the 1:1 line while the dashed lines mark the 10 % particle uncertainty range.

Cabauw (CES) CCN data

At CES the CCN number concentration is strongly underestimated, and the underestimation increases with increasing supersaturation. Fig. S2 shows examples of the closure attempt based on the κ-Köhler theory as described in Section 2.3.2 in the manuscript for SS = 1.0, 0.5 and 0.2 %. The results suggest that small particles, activating at higher supersaturation, were not sufficiently accounted for by the CCNC while they were measured by the SMPS. SMPS data have been quality controlled (Schlag et al., 2016). As this was not due to insufficient droplet growth to the detection limit of 1 µm of the optical particle counter in the CCNC, the bias most likely originated from particle losses in the sampling line to the CCNC. These size dependent losses could not be corrected for in retrospect. Hence, the dataset has not been corrected.

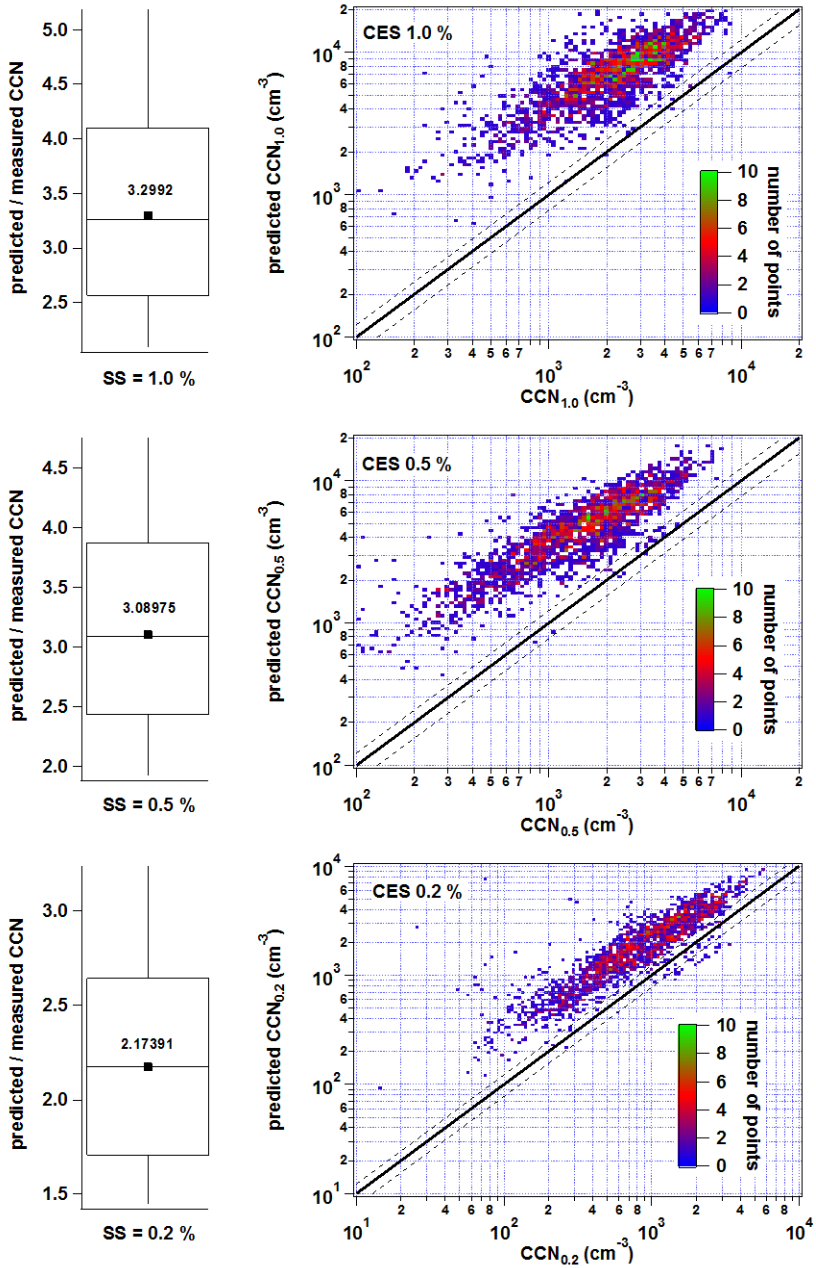

Fig. S2: Performance of closure study for the CES data set at SS = 1.0, 0.5 and 0.2 %. The left panels show the ratio of the predicted CCN number concentration based on the κ-Köhler theory and the measured CCN number concentration as a box and whiskers plot. The box indicates the interquartile range, the whiskers the 10th and 90th percentiles, the middle horizontal bar the median and the marker the geometric mean whose value is also given. The right panels show the relationship between the predicted and measured CCN number concentrations within logarithmic bins. The color code indicates the number of particles falling within one bin space. The solid black line is the 1:1 line while the dashed lines mark the 10 % particle uncertainty range.

2 Sensitivity study

Figure S3 demonstrates how the prediction skill of the CCN number concentration changes across a range of supersaturations when varying a number of parameters based on the corrected JFJ data. Panels a) and b) show in detail how the slope and correlation coefficient of the closure based on the κ-Köhler theory change assuming internally mixed particles. Changing the κ-value by a factor of two would introduce a bias of 15 % on average, panel d). If the supersaturation were calibrated incorrectly for the CCNC, for example by an exaggerated overestimation of 50 %, the predicted CCN number concentration would be roughly 20 % too high. Accounting for a potential, but again exaggerated, error in the size distribution measurements by shifting it by 20 % of the measurement range, i.e. overestimating the diameter by roughly 120 nm, 30 % more CCN would be predicted. If the surface tension were significantly lower, an assumed 50 %, the overprediction of the CCN number concentration would be around 40 %. A particle number counting error, evenly distributed across the whole size range, is directly proportional to the over- or underprediction of the CCN number concentration. Here an example for 10 % overcounting is provided.

Given that only exaggerated deviations of all parameters, but the particle counting, lead to moderate over- or underestimations of the CCN number concentration, these results suggest that precise counting of particles by both the SMPS and CCNC is most important. A 10 % deviation is within the expected uncertainty. Higher deviations will, however, be reflected proportionally in the results, as was the case at JFJ as shown in Fig. S1.

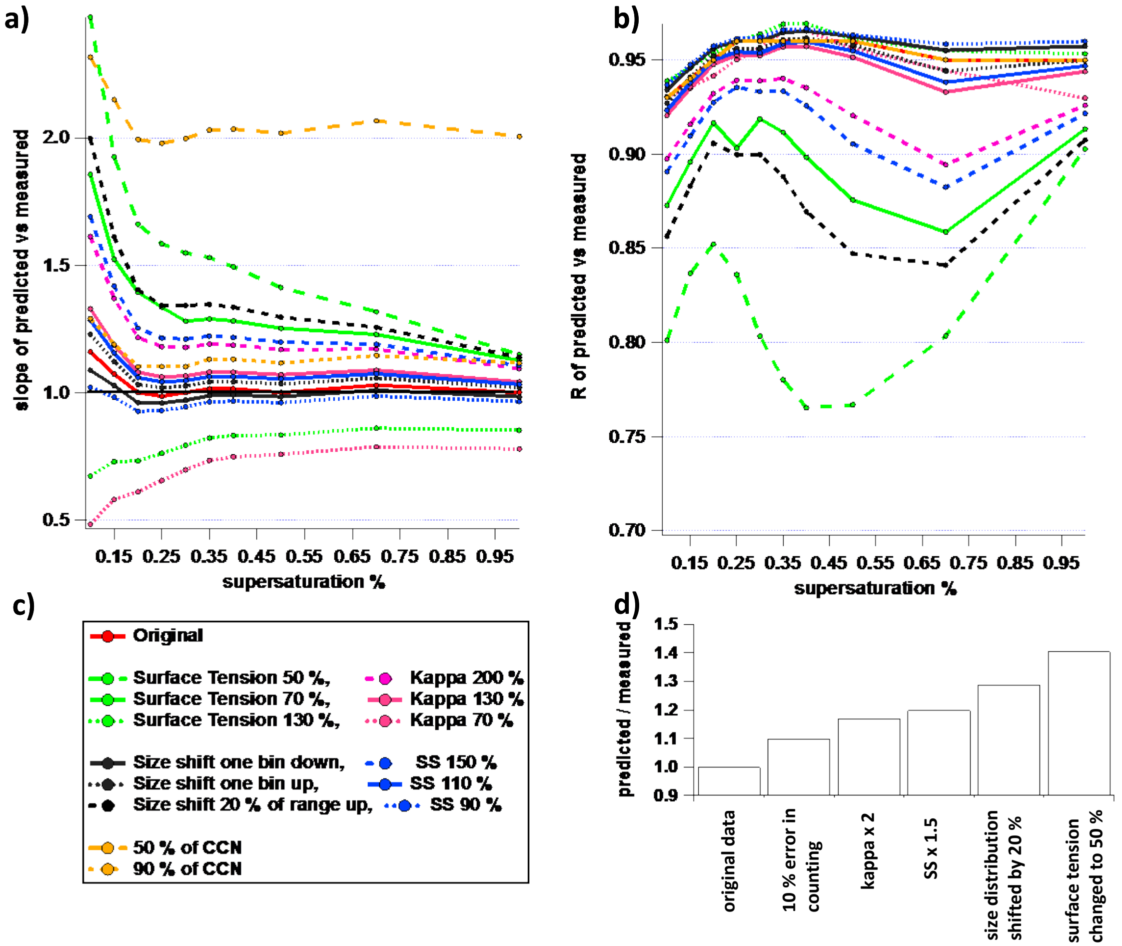

Fig. S3: Sensitivity analysis of a κ-Köhler closure study based on the uncorrected JFJ data. Panel **(a)** shows how the agreement between the predicted and measured CCN number concentration changes with supersaturation in form of the slope of the linear regression. Panel **(b)** shows the same for the correlation coefficient. The legend is given in panel **(c)**, while **(d)** summarizes the top panels by showing how the prediction skill changes for the SS = 0.5 % case when varying specific variables by extreme values.

3 Seasonal total particle number concentration and activation ratios

Figure S4 shows the total particle number seasonal cycle for all stations.

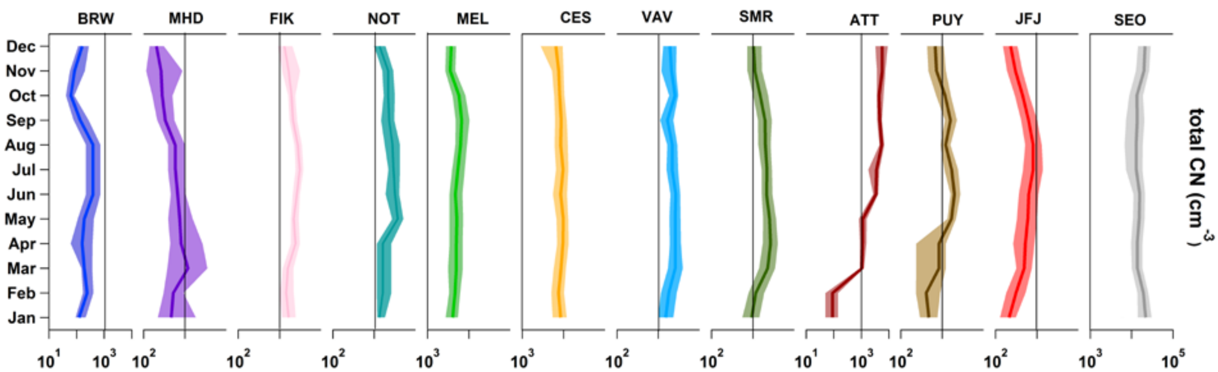

Fig. S4: Seasonal cycle of the total number concentration. The thick colored lines indicate the median value, while the shaded colored areas show the interquartile range. The black vertical bars indicate 1000 particles cm^{-3}.

Figure S5 shows the monthly variation of the fraction of activated particles (activation ratio “AR”). Note, based on the discussion in SI Sec.1 the *AR* for CES is underestimated and should be referred to with caution.

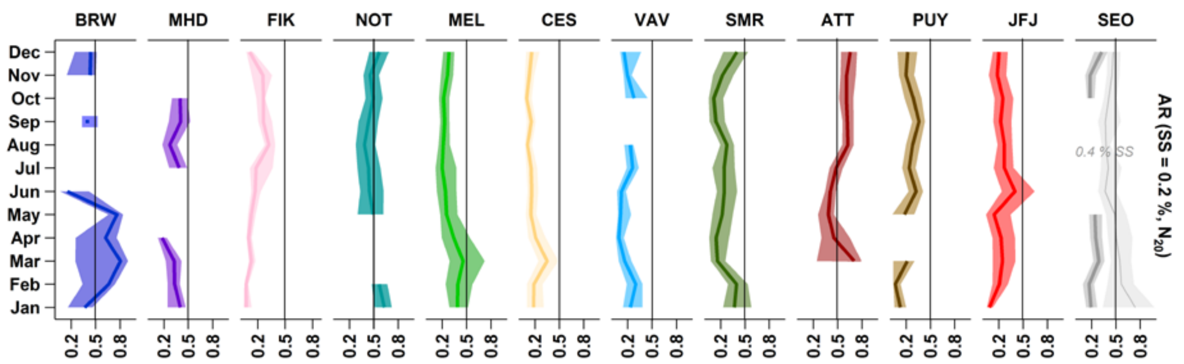

Fig. S5: Annual cycle of the CCN activation ratio at SS = 0.2 %. The basis for the total particle number is N_{20}. The thick colored lines indicate the median activation ratio, while the shaded colored areas show the interquartile range. The black vertical bars indicate 50 % activation. Due to higher data coverage in SEO results for SS = 0.4 % are shown additionally.

References

Herrmann, E., Weingartner, E., Henne, S., Vuilleumier, L., Bukowiecki, N., Steinbacher, M., Conen, F., Collaud Coen, M., Hammer, E., Jurányi, Z., Baltensperger, U., and Gysel, M.: Analysis of long-term aerosol size distribution data from Jungfraujoch with emphasis on free tropospheric conditions, cloud influence, and air mass transport, Journal of Geophysical Research: Atmospheres, 120, 9459-9480, 2015.

Jurányi, Z., Gysel, M., Weingartner, E., Bukowiecki, N., Kammermann, L., and Baltensperger, U.: A 17 month climatology of the cloud condensation nuclei number concentration at the high alpine site Jungfraujoch, Journal of Geophysical Research: Atmospheres, 116, n/a-n/a, 2011.

Schlag, P., Kiendler-Scharr, A., Blom, M. J., Canonaco, F., Henzing, J. S., Moerman, M. M., Prévôt, A. S. H., and Holzinger, R.: Aerosol source apportionment from 1 year measurements at the CESAR tower at Cabauw, the Netherlands, Atmos. Chem. Phys., 16, 8831-8847, 2016.

Schmale, J., Henning, S., Henzing, B., Keskinen, H., Sellegri, K., Ovadnevaite, J., Bougiatioti, A., Kalivitis, N., Stavroulas, I., Jefferson, A., Park, M., Schlag, P., Kristensson, A., Iwamoto, Y., Pringle, K., Reddington, C., Aalto, P., Äijälä, M., Baltensperger, U., Bialek, J., Birmili, W., Bukowiecki, N., Ehn, M., Fjæraa, A. M., Fiebig, M., Frank, G., Fröhlich, R., Frumau, A., Furuya, M., Hammer, E., Heikkinen, L., Herrmann, E., Holzinger, R., Hyono, H., Kanakidou, M., Kiendler-Scharr, A., Kinouchi, K., Kos, G., Kulmala, M., Mihalopoulos, N., Motos, G., Nenes, A., O'Dowd, C., Paramonov, M., Petäjä, T., Picard, D., Poulain, L., Prévôt, A. S. H., Slowik, J., Sonntag, A., Swietlicki, E., Svenningsson, B., Tsurumaru, H., Wiedensohler, A., Wittbom, C., Ogren, J. A., Matsuki, A., Yum, S. S., Myhre, C. L., Carslaw, K., Stratmann, F., and Gysel, M.: Collocated observations of cloud condensation nuclei, particle size distributions, and chemical composition, Scientific Data, 4, 170003, 2017.